Review article

Germanate glass for laser applications in ~ 2.1 μm spectral region: A review

Mamoona Khalid [*], Muhammad Usman, Irfan Arshad

Photonics and Communications Lab, Electrical Engineering Department, University of Engineering and Technology, Taxila, Pakistan

ARTICLE INFO

ABSTRACT

The growing landscape of laser applications in ~ 2 μm spectral region leads to the development of novel transparent media that provide low attenuation solutions for high power laser applications. This includes investigating glassy media such as heavy metal oxides (e.g. tellurite and germanate), fluoride and chalcogenides as an alternative to the most efficient and widely utilized silica glass. This review article discusses the potential of a heavy metal oxide lead-germanate glass (GeO_2-PbO-Ga_2O_3–Na_2O) for ~ 2.1 μm laser applications, with a focus on our contribution to the field. Firstly, a comparative study of commercially available silicates and fluorides with germanate glass is presented to reveal germanate to be a favorable material for 2.1 μm laser applications. Secondly, as our contribution to the field, we present the development of the first ~ 2.1 μm small cavity single frequency laser action in a Ho^{3+} doped GPGN glass that verifies its capability for ~ 2 μm laser applications and beyond.

1. Introduction

Laser light generation and amplification in ~ 2.1 μm spectral domain is of high importance these days for multiple novel applications as in absorption spectroscopy for detection of pollutants in the atmosphere; remote sensing; LiDAR; optical signal processing; micromachining; quality control; and in the defense [1,2]. ~ 2.1 μm wavelength lies in the eye safe region and is therefore gaining popularity in a number of medical applications as well. The large absorption coefficient of water around ~ 2.1 μm has opened new era of highly precise laser surgery with excellent thermal management. The result is localized ablation of tissue with a small injury zone of ~ 0.5 mm compared to the conventional lasers operating in the shorter wavelengths (up to 1.5 μm) for laser surgery. Moreover, in contrast to the other laser systems, ideal coagulation depth of as small as 0.1–0.2 mm results from ~ 2.1 μm laser exposure [3]. This type of laser surgery helps preventing post-surgical complications in patients as it starts the coagulation process (transition from liquid blood to semi-solid blood clot) as soon as the tissue is exposed to ~ 2.1 μm radiations. The procedure, therefore, suppresses the bleeding and leads towards a smooth and efficient surgical process [3].

The rare earth (RE) ions that have the ability to emit around 2.1 μm are the Tm^{3+} (Thulium) and Ho^{3+} (Holmium). For around 2.1 μm laser radiations the emission spectrum of Tm^{3+} ranges between 1.7 μm–2.1 μm. On the contrary, Ho^{3+} ion emits within the wavelength range 1.8 μm–2.3 μm. There are, however, some major advantages of Ho^{3+} ion over Tm^{3+} ion including, (i) almost four times higher emission cross-section of Ho^{3+} compared to Tm^{3+} around 2.1 μm [5] (Fig. 1(a)), (ii) Although Tm^{3+} is a very efficient ion (pumping wavelength ~ 0.8 μm) and high power Tm^{3+} fiber lasers (λ ~ 1.9 μm) have already been developed and commercialized,

---

* Corresponding author.
E-mail address: mamoona.khalid@uettaxila.edu.pk (M. Khalid).

however, their lasing wavelength of ~ 1.9 μm has restricted transmission in the atmospheric transmission window (Fig. 1(b)) and therefore have some limitations (from an application point of view) compared to Ho^{3+} lasers (operating wavelength of Ho^{3+} ~ 2.1 μm).

The excitation wavelengths of a specific rare-earth ion are usually determined by collecting their absorption spectrum over a range of wavelengths. The multiple ground state energy bands of Ho^{3+} in a specific germanate glass (GPGN) ranging from 0.2 μm to 3.3 μm is depicted in Fig. 2(a). It can be observed from Fig. 2(a) that the Ho^{3+} ion has multiple energy bands showing peaks at $^5F_1+^5G_6$ (0.45 μm), $^5F_4+^5S_2$ (0.54 μm), $^5F_5$, $^5I_5$ (1.15 μm), $^5I_6$ and $^5I_7$. For ~ 2.1 μm laser radiations $^5I_7$ absorption band is considered which ranges from 1.8 μm to 2.3 μm. Two pumping schemes are normally utilized for the development of ~ 2 μm Tm^{3+} and Ho^{3+} lasers i.e. (i) non-resonant pumping scheme where the quantum defect between emission spectrum and absorption spectrum of the laser ion is large such that there is no overlap between them for the laser ion (e.g., using a laser diode (LD) operating at ~ 1.2 μm for 2.1 μm radiations in Ho^{3+} laser ion, as in Fig. 2(b)). This type of pumping scheme is cost effective as it allows utilizing readily available pump sources with high power scalability readily available with high power scalability, (ii) In-band resonant pumping where the emission band overlaps the absorption band of the laser ion (e.g., 1.95 μm Ho^{3+} excitation via a thulium fiber laser for 2.1 μm laser emission, Fig. 2(c)). In-band pumping is rather efficient compared to non-resonant pumping scheme, however, unavailability of cost-effective high-power laser diodes at longer wavelengths makes the process challenging to be considered.

The ~ 2.1 μm resonant $^5I_7$ absorption band of Ho^{3+} suggests utilizing a Tm^{3+} fiber laser operating at 1.95 μm as pump source due to its strong absorption cross section compared to other wavelengths in the $^5I_7$ absorption band. Non-resonant excitation for ~ 2.1 μm laser emission for Ho^{3+} is generally achieved using high power laser diodes operating at 1.15 μm. The high-power pumping LDs operating at the mentioned wavelengths are costly and their commercial availability is uncommon. Adding a sensitizer ion (donor) to the laser ion (acceptor) provides an alternative solution to utilize available high-power LDs [6]. Relevant sensitizers that can be doped with the active ion (Ho^{3+}) to achieve 2.1 μm laser operation include Tm^{3+}, Pr^{3+}, Er^{3+}, or Yb^{3+}.

Novel soft glasses are currently under investigation to support the expanding laser applications in ~ 2.1 μm spectral region. The three soft-glass families widely being explored for laser applications include heavy-metal fluorides (HMF) [7], heavy-metal oxides (HMOs) and chalcogenides [8]. Extensive research on HMO glasses (e.g. germanate [9] and tellurite [10])) reveals their potential as a promising material for ~ 2.1 μm novel laser applications. This review article investigates the capability of a novel lead-germanate glass possessing chemical composition GeO_2-PbO-Ga_2O_3–Na_2O (hereafter referred to as GPGN glass) for lasing applications around 2.1 μm spectral region in contrast to commercially existing silica and non-silica glasses.

## 2. Characteristics of gain media for laser applications

Selection of an appropriate gain medium for laser applications is the most crucial part of the laser engineering process. Each gain medium is rigorously evaluated through detailed spectroscopic analysis before it can be utilized for laser applications. A few of the characteristic parameters of a high gain laser material are listed below [11–15].

   i. High thermal, chemical, and mechanical stability with high damage threshold values (for sustained high power laser delivery)
   ii. Low phonon energies (to minimize non-radiative decay process to achieve high laser efficiencies)
   iii. High transparency and low attenuation in the spectral region of interest (to achieve higher laser efficiency)
   iv. The ability to accommodate large concentrations of dopant ions (for high laser efficiencies in micro-scale sample lengths).

The transition temperature of glassy medium (T_g) and its coefficient of thermal expansion (κ) usually defines its durability and its mechanical strength. Other properties to identify the laser durability and rigidness (and therefore the damage threshold of a material)

(a)   (b)
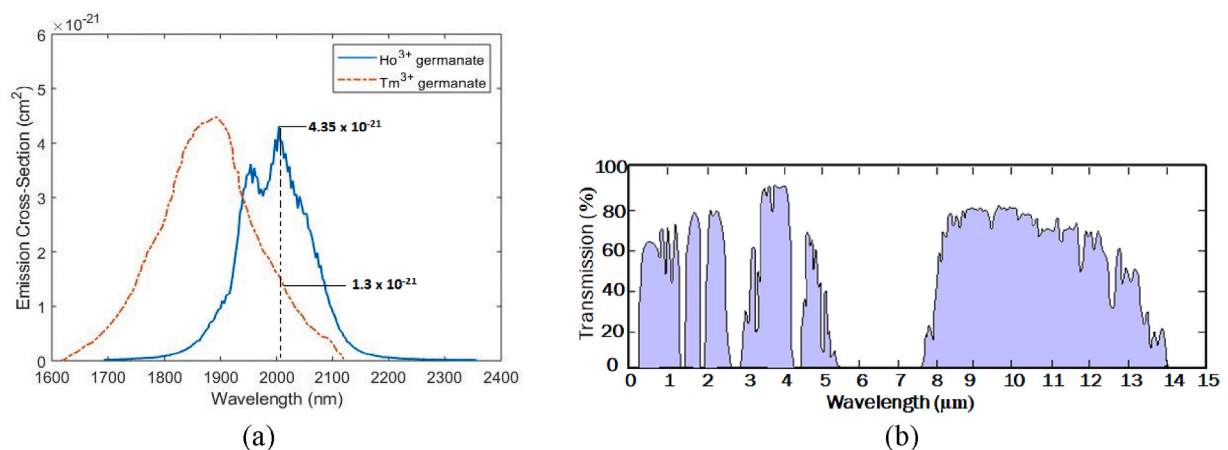
Fig. 1. (a) Cross-section for ~ 2 μm emission in Tm^{3+} and Ho^{3+} laser ions in germanate glass. (b) Atmospheric transmission window with ~ 2 μm providing maximum transmission in the atmosphere [4].
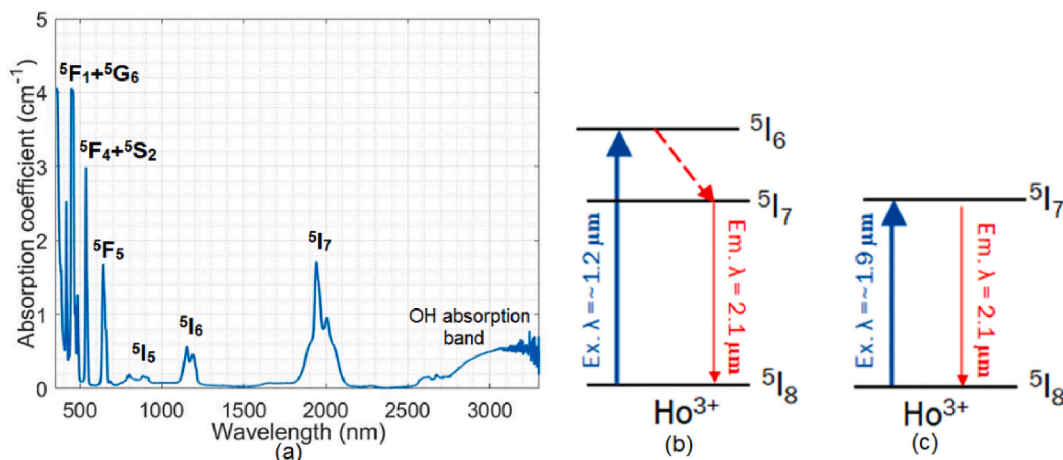
Fig. 2. (a) Absorption spectrum of Ho^{3+} in GPGN from 400 nm to 3300 nm. (b) Non-resonant pumping scheme for Ho^{3+} using a ~1.2 μm laser diode (LD) (c) Resonant pumping scheme for Ho^{3+} using ~ 1.9 μm Tm^{3+} fibre laser.

are the fracture toughness, Knoop hardness, Poisson's ratio, Youngs modulus etc.

2.1. Silicates

Silica (SiO_2) is abundantly available in nature which after processing (glass fabrication) becomes well equipped with the above-mentioned properties for only up to ~ 2 μm spectral region. Silica glass comprises of propagation loss as low as 0.02 dB/cm at 1550 nm [16] and possesses low thermal expansion coefficient which makes them extremely attractive for high power laser applications and for fiber drawing at higher temperatures. Silicates retain high damage threshold values of ~ 500 MW/cm^2 [12] that makes them suitable for high power laser operations (mostly fiber lasers) ranging up to ~ 2 μm [11,17]. As an example, authors record high laser slope efficiency of 43% at an extended Ho^{3+} wavelength of 2.11 μm in a Tm^{3+}/Ho^{3+} silica-based fiber laser that can attain maximum of 83 W output power [18].

The robust covalent structure of silicates has strong bonding between its atoms. Their high energy bandgap (E_g) of ~ 9 eV [19] makes them mechanically, thermally and chemically more durable [20,21] compared to any other available glass material. To date, silicates (silica glass) are the most successful laser host materials up to 2 μm [11]. However, going further into the mid-IR spectral region their efficiency compromises because of their elevated phonon energy of ~ 1100 cm^{-1} and strong water absorption above ~ 2 μm. To mitigate this issue [22] proposes a solution of lowering the phonon energy of the medium using a hybrid composition of germanate (GeO_2) and silica to enhance its ~ 2.1 μm emission properties while keeping the thermal stability of silica for high power laser operations. Similarly, in Ref. [23], authors add GeO_2 in a silica glass to enhance its ~ 2.1 μm emission properties and suppress the losses that occur due to the high concentrations of hydroxyl ions (OH) present in silica glass. Studies in [24] follow a similar approach of modifying the glass for enhanced ~ 2.1 μm emission by adding GeO_2 in a Yb^{3+}/Ho^{3+} co-doped silica glass to lower its phonon energy while keeping intact the properties of silica itself. Some studies like in Ref. [25] have also reported enhanced ~ 2.1 μm laser efficiency in a Yb^{3+}/Ho^{3+} co-doped phosphate glass using the similar approach of modifying the glass with fluoride. Overall, it is observed that the laser capability of silica glass can be slightly extended above 2.1 μm by modifying the glass composition to lower its phonon energy.

Table 1 compares different optical characteristics of commercially available silica and ZBLAN glass with the recently investigated lead-germanate glass (GPGN) for laser applications. Research shows that germanate possesses higher thermal and mechanical properties compared to ZBLAN but lower compared to silica (Table 1). Moreover, germanate possess medium phonon energies which make them attractive in contrast to silica for ~ 2.1 μm laser applications.

Table 1
Optical properties of germanates compared to silica, and fluoride glass.

Glass Property	Silica [26]	ZBLAN [26]	GPGN [27–31]
Approximate transmission range (μm)	0.16–4.0	0.22–5.0	0.3–6
Phonon energy (cm^{-1})	1100	600	800
Transition temperature (°C)	1175	260	390
Thermal conductivity, W/(m·K)	1.38	0.63	0.7
Density (g/cm^3)	2.2	4.33	5.63
Refractive index (@ 0.589 μm)	1.458	1.499	1.835
Nonlinear index (10^{-20} m^2/W)	2.87	2.38	56
Thermo-optic coefficient (10^{-6}/K)	11.9	−14.75	9

2.2. Fluorides

Among the soft glass family, fluorides such as fluorozirconate (ZBLAN) present excellent lasing properties in short to mid infrared spectral region. ZBLAN glass composition possesses low vibrational energy (~ 550 cm^{-1}) and broader mid infrared transmission range compared to silica and HMO glasses. They are considered efficient gain media for laser applications in the short to mid-IR spectral region in comparison to the other exotic glasses. Researchers have extensively investigated single and multiple doped fluoride glasses with rare earth ions (e.g. Er^{+3}, Pr^{3+}, Dy^{+3}, Tm^{+3}, Ho^{+3} etc.) to determine their lasing capability as waveguide and fiber lasers ranging from ~ 1 μm to 3.9 μm [32–36].

Efficient watt level laser radiations at ~ 2.1 μm have been successfully demonstrated in fluoride glasses doped with Tm^{3+} and Ho^{+3} [35,37,38]. Sensitizing Ho^{3+} with Pr^{3+} has realized efficient lasing up to 3.5 μm [39]. ~ 4 μm lasing capability of ZBLAN has also been reported when doped with Dy^{3+} [36]. In fact, among the soft glass materials being investigated for laser operation in infrared region, ZBLAN are only ones to date to successfully demonstrate lasing up to ~ 4 μm (Fig. 3).

The potential of ZBLAN is further investigated spectroscopically for lasing wavelengths above 4 μm. However, the longer transitions farther above shortwave infrared region are difficult to achieve as the difference between the relevant energy states with respect to their ground levels are quite large. In other words, longer wavelengths have large quantum defects which require multiple high power excitation sources that are challenging to achieve using the readily available high-power LDs.

Fig. 3 presents an exponentially decreasing trend in optical power received at the output with respect to the emitted wavelength for different laser ions [40]. It is observed that as we approach to the mid-IR region, the laser efficiency drops exponentially. A few of the factors affecting the laser power in longer wavelengths are mentioned below and research is required to mitigate these issues in order to generate efficient pump sources for longer wavelengths [40].

  i. Reduced transmission (%T) of the glass in the mid-IR spectral region.
 ii. High phonon energy of the medium. The longer laser transitions are affected by multi-phonon decay and other non-radiative processes such as OH absorption above 2 μm, up-conversion and excited state absorption (ESA).
iii. The gain media for longer transitions are still under investigation and thus immature.
 iv. The unavailability of high-power sources to pump the longer transitions.

Despite their wider lasing capability in the mid-IR region, the thermal stability (ΔT) of ZBLAN towards crystallization is low compared to silicates and germanates (e.g. GeO_2-PbO-Ga_2O_3–Na_2O (GPGN) glass) (Table 2) and is more prone to contamination by oxygen ions [41]. The difference in crystallization temperature (T_x) and the transition temperature (T_g) of a medium generally provides its thermal stability i.e., $\Delta T = T_g - T_x$. Moreover, handling ZBLAN fibers is quite challenging due to their brittle nature, low chemical stability and poor mechanical strength (Table 1) [31]. Inscription of waveguides in ZBLAN glass for waveguide laser applications is also a complex process due to their negative dn/dt value. Negative dn/dt even makes it complicated to achieve microchip laser operation in ZBLAN.

Table 3 presents the ~ 2.1 μm laser capability of singly doped Ho^{3+}: ZBLAN waveguides for both non-resonant and resonant pumping schemes. It is observed that the highest ~ 2.1 μm laser slope efficiency of $\sim 51\%$ is achieved when Ho^{3+} is resonantly pumped with a Tm^{3+} fiber laser. The reason being the small quantum defect between the pump and laser wavelength for efficient energy migration. Ho^{3+} when synthesized with Tm^{3+} ion in ZBLAN waveguides is only 29% efficient. The possible causes include the energy loss due to the quenching factors such as up-conversion (UC) and excited state absorption (ESA) due to the presence of a number of energy states in both ions. These factors generally increase the heating load on the co-doped laser system, quench the lifetime of $^5I_7$ energy state and hence affects the $^5I_7 \rightarrow {}^5I_8$ laser emission. Singly doped Tm^{3+} in ZBLAN on the other hand is up to 67% efficient due to the well-known cross relaxation achieved in Tm^{3+}. However, its emission wavelength is slightly below 2 μm (~ 1.95 μm laser emission)
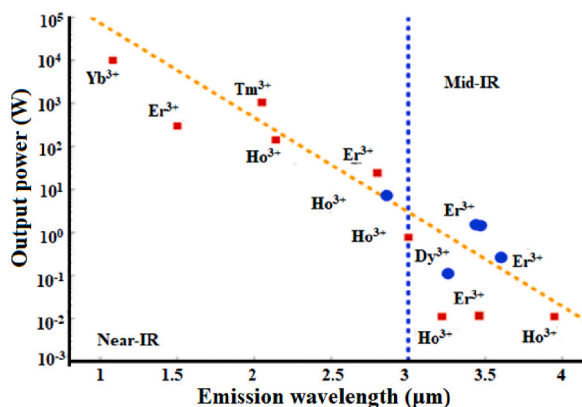

Fig. 3. Exponentially decreasing trend in the received optical power with respect to the emitted wavelength for different laser ions in ZBLAN [40]. The high-power region before dotted blue partition (~ 3 μm) is near to short infrared region while after ~ 3 μm is the mid-IR spectral region.

Table 2

Differential Scanning Calorimeter (DSC) readings depicting thermal stability (ΔT) for various glasses.

Glass material	Glass transition temperature, T_g (°C)	Glass crystallization temperature, T_x (°C)	Thermal stability, [ΔT (°C) $= T_x - T_g$]	Ref
Oxyfluoride	570	712	142	[42]
Silicate (SPKBEH)	425	585	160	[43]
Phosphate	410	500	90	[42]
Tellurite	348	495	147	[42]
Other Germanate	685	808	123	[42]
Silicate (SBLHY)	620	799	179	[42]
GPGN	390	No definite crystallization peak	No crystallization	[44]
Chalcogenide	125	400	275	[45]
ZBYA fluoride	332–350	428–449	96–99	[46]
ZBLAN	250	400	150	[47]

Table 3

Ho^{3+} doped fluoride (ZBLAN) glasses for $\sim$ 2 μm laser operation.

Glass Material	Pump Source	Pump wavelength, λ_P (nm)	Threshold power, P_{th} (mW)	Laser wavelength, λ_L (nm)	Output power, P_{out} (mW)	Laser slope efficiency, η_s (%)	Ref
Ho^{3+}: ZBLAN	Diode	1150	28	2900	27	20	[48]
Ho^{3+}: ZBLAN	Tm f. Laser	1945	180	2070	1100	51	[38]
Tm^{3+}/Ho^{3+}: ZBLAN	Ti: Sa	790	75	2100	25	29	[49]
Tm^{3+}/Ho^{3+}: ZBLAN	Ti: Sa	790	20	2052	76	20	[37]
Tm^{3+}: ZBLAN	Diode	790	21	1880	47	50	[49]
Tm^{3+}: ZBLAN	Ti: Sa	790	75	1900	132	50	[37]
Tm^{3+}: ZBLAN	Diode	791	265	1900	60	54	[50]
Tm^{3+}: ZBLAN	**Ti: Sa**	**790**	**12**	**1890**	**205**	**67**	[51]

(Table 3).

2.3. Heavy metal oxide

Silica [52] and fluoride [53] glasses have widely been researched for small cavity laser operations in near to mid infrared spectral region. The enhanced thermal stability and high fracture tolerance of silica in comparison to any other gain material reported earlier makes them attractive host for waveguide and microchip laser operations for only up to 2 μm. The transmission above $\sim$ 2 μm in silica glass significantly reduces due to multiple factors, therefore, its use in laser applications (above 2 μm) is limited [54,55]. In contrast to silica, the transmission spectrum of fluorides (more specifically ZBLAN) extend wider into the mid-IR region and also have relatively lower phonon energies ($\sim$ 600 cm^{-1}) compared to silica and HMO ($\sim$ 750 - 850 cm^{-1}) [56]. In fact, to date the only mid-IR lasers are practically demonstrated in ZBLAN (up to 3.9 μm) [57]. However, the lower thermal conductivity and mechanical strength of fluorides (due to lower glass transition temperature, T_g) make them difficult to work with, especially for small cavity bulk laser development (e. g. disk lasers) as fluorides are more fragile and have the tendency to fracture easily.

Research on soft glasses for mid infrared laser applications now a days have focused more on the exploration of HMO glasses which includes germanate and tellurite as active laser material [58]. This is because HMO glasses have presented promising laser results with many advantages over silicates and fluorides [31,44,59,60]. Within the HMO, germanate possess comparable mechanical and thermal properties with the commercially available silica glasses and offer advantage over widely researched tellurite glasses [31,44,61]. A few of the distinctive properties of germanate in comparison to silicate, are its higher linear and nonlinear refractive indices, medium levels of phonon energies, and a wider transmission up to $\sim$ 6 μm. These characteristics all together make germanate an attractive gain medium for laser applications as well as for nonlinear applications such as supercontinuum generations and four wave mixing etc. [62].

Fluorescence spectroscopy of HMO glasses doped with Dy^{3+} (pumping at 808 nm) is investigated in Ref. [63] for 3 μm–4 μm mid-IR spectral region. It is concluded in the study that the emission cross section of Dy^{3+} in HMO is much larger compared to that of Dy^{3+}: ZBLAN which reflects that higher gain is more likely to be achieved in HMO glasses. However, their practical implementation is yet to be demonstrated and are quite challenging, most probably due to their higher phonon energies (700–800 cm^{-1}) and higher multi-phonon decay rates in short to mid-IR spectral region when compared to ZBLAN. In short, despite being brittle and having inferior thermal stability compared to HMO glasses, ZBLAN still stands alone in competition for mid-IR lasing applications up to $\sim$ 4 μm.

Research on germanate glasses reflects that this glass is a good compromise of the characteristics vital for laser applications up to and beyond $\sim$ 2.1 μm [54]. Their wider transparency in short to mid-IR spectral region along with their higher thermal and mechanical strengths have made germanates an attractive alternate for high energy laser systems [64]. Moreover, their ability to accommodate

large concentrations of dopant ions make them fascinating for small cavity (waveguides and micro-chip) laser operations [54]. The high ion accommodation capability of germanate glasses is evident from the fact that high power germanate fibre lasers (4 wt % Tm^{3+} doped) with efficiency as high as 68% for ~ 2 μm laser have already been developed resulting in high output power of ~ 104 W in just a 40 cm long fibre [65]. In addition to this, only 2 cm long efficient fibre lasers with ~ 35% slope efficiency for ~ 2 μm laser operation have also been reported [66]. Higher ion concentration results in utilizing small sample lengths for achieving highly efficient lasers.

High emission cross-sections σ_{ems} (λ) of different dopant ions (e.g. Tm^{3+} [67] and Ho^{3+}) are also observed in germanate glass (compared to the fluoride glass, e.g. ZBLAN) due to their higher refractive index. This can be justified by the direct relation of σ_{ems} to the refractive index of the glass i.e. $\sigma_{ems}(\lambda) \propto n^3$ [67]. High refractive index of germanate glass (n = 1.8 − 2) suggest strong absorption of the pump radiations within a specific sample length due to higher electric dipole interaction and thus achieving high oscillator strength for a specific absorption band [67]. The reduction in sample size due to higher refractive index (and large mode areas of bulk lasers) also increases the threshold for nonlinear effects such as Brillouin and Raman scattering. These nonlinear scattering effects are more prominent for longer sample lengths (as is the case in fibres) and when high intensities are achieved using small core areas. Efficient lasing in silica or ZBLAN fibre lasers for such short fibre lengths (e.g. 2 cm fiber as in Ref. [66]) have not yet been reported.

Among the HMO glasses, zinc-tellurite glasses have been extensively researched for laser applications due to their low phonon energy (~ 750 cm^{-1}) [31,44,68,69]. However, their low thermal stability against crystallization lead to the investigation of germanate glasses. Lead-germanate glass, a member of the germanate glass family, is of particular interest for mid infrared laser applications as it offers comparable phonon energy as zinc-tellurite glasses [31,44,68,69]. Lead germanate glass possesses higher thermal, chemical, and mechanical stability among tellurite and other germanate glasses and therefore are considered to be promising alternative for the development of low-loss fibre and waveguide lasers in mid infrared spectral region [44].

Due to their superior chemical and thermal stability as compared to other mid-IR transmitting glasses, lead-germanate glasses are interesting host materials for 2 μm laser applications. These glasses are also viable choice for the production of optical components (e.g. lenses) because of their higher refractive index compared to other glasses in the germanate family [31,70–73]. High-power non-linear applications and dispersion compensation both benefit from high refractive index (e.g. broadband supercontinuum generation and four-wave mixing). Lead-germanate glass also has the ability to hold significant concentrations of dopants, which makes it an appealing option for single frequency laser operations when short cavity lengths with enough net gain are essential [74].

Within the lead germanate glasses GPGN glass is one of the most comprehensively researched mid infrared glass having composition $56GeO_2$-$31PbO$-$4Ga_2O_3$–$9Na_2O$ and broad transmission spectrum [44]. The wider transmission of GPGN glass into the mid infrared region helps considering broad range of laser wavelengths. When compared to the well investigated BaO-Ga_2O_3-GeO_2 germanate glass (BGG), which melts at 1500 °C [75], GPGN glass melts at relatively lower temperature of 1200°C–1250 °C [44,55,56]. This allows for rapid fabrication of GPGN in research facility in a dry atmosphere utilizing a glovebox-based melting facility.

The $^5I_7$ fluorescence lifetime, τ_r, of Ho^{3+} in GPGN is longer (~ 7.7 ms) compared to that of silica glass (~ 1.3 ms). One of the many factors enhancing the radiative lifetime of Ho^{3+} in GPGN (~ 800 cm^{-1}) is its low phonon energy of ~ 800 cm^{-1} compared to silica glass (1100 cm^{-1}). Longer lifetime of GPGN indicates higher population inversion and thus high gain can be expected for ~ 2 μm laser. Fig. 4 [75] compares the transmission properties of germanate with silica and other glasses. It can be observed that germanate glass is transparent in the mid-IR region up to ~ 5.5 μm (Fig. 4(a) (green)). The same is true for GPGN glass as illustrated by the FTIR transmission spectrum (Fig. 4(b)) of a Yb^{3+}/Ho^{3+} co-doped GPGN glass [54] where the wide dip from 1.8 μm to 2.2 μm is the $^5I_7$ absorption band of Ho^{3+} and the dip from 2.8 μm to 3.3 μm is the OH absorption band.

3. Ho^{3+} doping for ~ 2 μm laser application

Earlier demonstration of Ho^{3+} doped lasers in commercially available silica and fluoride glasses [76–80] revealed lower-than-expected slope efficiencies compared to their theoretical counterparts. This was observed to be true for both in-band and
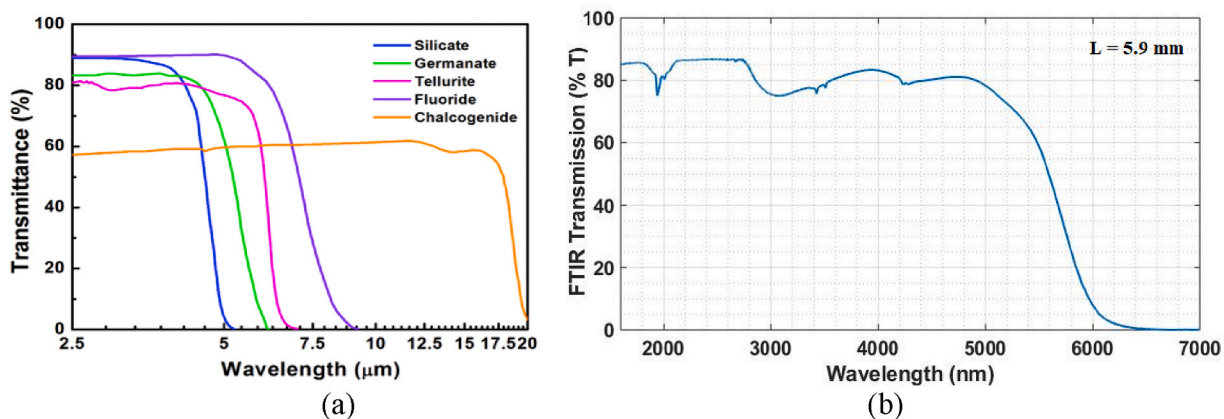

Fig. 4. (a) Comparison of transmission ranges for silica, fluorides, Heavy metal oxides (Telluride) and chalcogenide glasses [75]. (b) FTIR transmission spectrum for Yb^{3+}/Ho^{3+}: GPGN sample, high transparency achievable up to 5.5 μm for L = 5.9 mm long sample.

non-resonant pumping schemes. For non-resonant pumping the reported laser slope efficiencies are $\sim$ 50% [23] while the practical demonstrations have achieved up to only 37% [76,77]. In some cases where the slope efficiency exceeds 40% [78,79] the theoretical counterparts approaches >75%. In terms of in-band pumping the theoretical laser slope efficiency exceeds 90%, however, experimental measurements only return <65% efficiency [81,82]. Only in Ref. [80] the authors demonstrated a slope efficiency of $\sim$ 87% in a Ho^{3+} doped fiber laser system which is very close to its theoretical quantum efficiency (90%). All the mentioned lasers are Ho^{3+} doped silica or fluoride fiber laser systems and very few studies present the material response for small cavity laser (e.g., waveguide laser) applications using germanate glass as the gain medium.

Various rare earth (RE) doped germanate glasses have been researched spectroscopically for laser applications in visible to shortwave-IR spectral regions ($\sim$ 0.4 µm–2.5 µm). Earlier reported work on Ho^{3+} [83,84] and Tm^{3+} [65,85] doped germanate glass fiber lasers have demonstrated reasonably efficient laser slope efficiencies of $\sim$ 35% [83] and $\sim$ 68% [65], respectively. In this review article we only focus on Ho^{3+} based singly doped and co-doped laser systems in germanate for $\sim$ 2.1 µm laser applications.

3.1. Singly doped Ho^{3+} germanate laser systems

As mentioned earlier, germanate glasses have shown promising laser properties in different wavelengths of near to shortwave-IR spectral region. These results are mostly based on the spectroscopic studies and there is still a need to practically demonstrate the laser capability, power scalability, stability, and cost effectiveness of germanate glasses when used as gain media for laser applications, specifically around 2.1 µm spectral region.

Laser emissions around 2.1 µm can be achieved both by doping single Ho^{3+} ion in the glass or by adding sensitizer ions with Ho^{3+} (co-doping). A few theoretical studies identify up to 47% quantum efficiency in a resonantly pumped (using a 1.94 µm Tm^{3+} laser system) single Ho^{3+} doped lead germanate glass possessing a molar composition of $50GeO_2$-$5SiO_2$–$20PbO$–$20CaO$–$5K_2O$ (GSPCK) [23]. A high doping ion density of 6×10^{20} ions/cm^3 of Ho^{3+} is used in the study [23]. Similar composition of Ho^{3+} doped GSPCK glass was investigated experimentally by another group in Ref. [83] where the authors have achieved $\sim$ 35% laser slope efficiency around 2.1 µm. Similar composition of GSPCK in Ref. [85] with lower concentration of Ho^{3+} compared to Refs. [23,83] revealed a high theoretical quantum efficiency in the sample. In another work on germanate glass in Ref. [86], the authors claim a single frequency in-band pumped tunable laser operation with slope efficiency $\sim$ 68% in a 2 cm long heavily doped (4 wt%) Ho^{3+} germanate fiber (Table 4).

3.2. Co-doped Ho^{3+} germanate laser systems

In-band pumping of a gain medium usually generates high laser slope efficiencies because of the overlap between the excitation and the fluorescence spectrum of the laser ion. This overlap helps efficient energy migration among the ions. For longer laser transitions, high power pump sources are scarce and not always economical and therefore another approach is required where low-cost laser diodes can be utilized. Co-doping the laser ion with a sensitizer ion is a reasonable approach for such purpose. However, the probability of inducing thermal effects increases in the active material throughout the lasing process due to the involvement of a number of energy states of the laser ion (acceptor) and the sensitizer ion (donor). The selection of an appropriate sensitizer ion is therefore important to ensure maximum energy transmission from the sensitizer ion to the laser ion. For such purpose a donor ion whose absorption band preferably overlaps with one of the emission bands of the acceptor ion (for a specific laser transition) is generally recommended.

For $\sim$ 2.1 µm laser operation, Ho^{3+} is usually co-doped with Tm^{3+}, Yb^{3+} or Er^{3+} as sensitizer ions. Some theoretical spectroscopic studies have also reported the tri-doped [87,88] or four ion doping [89,90] in germanate glass for multi-wavelength tunable laser operation including 2.1 µm. The results for multiple ion systems are, however, not yet experimentally validated and there is still gap in knowledge in this area.

Table 5 presents the theoretical and experimental quantum efficiencies of $\sim$ 2.1 µm laser in a few of the co-doped germanate systems. A quantum efficiency of 79% is earlier reported in a GeO_2- BaF_2-Ga_2O_3–LiF glass where Ho^{3+} is co-doped with Yb^{3+} and excited using a 976 nm laser diode (Table 5). This co-doping generally promotes high energy transmission from Yb^{3+} ($^2F_{5/2}$) to different energy levels of Ho^{3+} [54,91] (e.g. most prominent energy transfer is to $^5F_4$, $^5F_5$ and $^5I_5$). [5] is also a Yb^{3+}/Ho^{3+} laser system with slightly different glass composition where the authors investigated the spectroscopic parameters of Ho^{3+} in the glass using Judd-Ofelt analysis. It can be observed from Table 5 that the highest quantum efficiency is estimated in GBGL glass, however, the results are not experimentally validated. On the contrary, both theoretical and experimental laser slope efficiencies have been determined in our previous work in a GPGN glass [54]. The experimental laser results in GPGN gives $\sim$ 20% laser slope efficiency which is much less than the theoretical estimation. This is because the laser cavity was not optimized for losses and anti-reflective coating was not applied on the end facets of the GPGN sample. However, the results indicate great potential of GPGN glass for $\sim$

Table 4
Singly doped Ho^{3+}: germanate laser systems.

Glass composition	Doping concentration (cm^{-3})	Spectroscopic quantum efficiency (%)	Laser slope efficiency (%)	Ref.
GeO_2-SiO_2-PbO-CaO-K_2O (GSPCK)	6×10^{20}	47%	–	[23]
GSPCK	6.3×10^{20}	–	35%	[83]
GSPCK	0.15×10^{20}	69%	–	[85]
Germanate	4 wt %	–	68%	[86]

Table 5
Co-doped Ho^{3+} laser systems in germanate sensitized with two or three dopant ions.

Glass composition	Doping ions	Pumping wavelength	Quantum efficiency = $A_{rad} \times \tau_m$	Laser slope efficiency (η_s)	Ref.
GeO$_2$- BaF$_2$-Ga$_2$O$_3$–LiF (GBGL)	Yb^{3+}/Ho^{3+}	976 nm LD	79%	–	[91]
GeO$_2$-BaF$_2$-Ga$_2$O$_3$–La$_2$O$_3$	Yb^{3+}/Ho^{3+}	976 nm LD	–	–	[5]
GeO$_2$-Ga$_2$O$_3$–BaO (BGG)	Tm^{3+}/Ho^{3+}	791 nm LD	–	4.7%	[92]
GeO$_2$-TeO$_2$-Nb$_2$O$_5$-YF$_3$	Yb^{3+}/Er^{3+}/Ho^{3+}	980 nm LD	47%	–	[87]
GeO$_2$-Ga$_2$O$_3$–Na$_2$O–BaO–La$_2$O$_3$	Tm^{3+}/Er^{3+}/Ho^{3+}	980 nm or 808 nm LD	50%	–	[88]
GeO$_2$-PbO-Ga$_2$O$_3$–Na$_2$O (GPGN)	Yb^{3+}/Ho^{3+}	976 nm	76%	20%	[54]

2.1 μm laser applications (provided the losses are minimized in the laser cavity).

One of the most important parameters that predicts the laser performance of an active material at a particular wavelength is its quantum efficiency (QE) which defines how many pump photons have been successfully converted to the laser photons. Theoretically, QE is the product of radiative transition probability, A_r, and the measured fluorescence lifetime (τ_m) of $^5I_7$ energy state of Ho^{3+}. Radiative lifetime, τ_r, is estimated spectroscopically from the radiative transition probability of $^5I_7$ energy state (i.e., $\tau_m = 1/A_r$), while τ_m is the fluorescence lifetime which is determined through the time resolved fluorescence spectroscopy.

In terms of other co-doped laser systems, ~ 2.1 μm laser operation is observed in a barium-gallo-germanate (BGG) glass in Ref. [92] where Ho^{3+} is co-doped with Tm^{3+}. The attained laser slope efficiency in Ref. [92] is only 4.7% when pumped with a 796 nm laser diode. Although the well-known cross-relaxation process in Tm^{3+} leads to an energy transfer efficiency of ~ 63% towards Ho^{3+}, yet the very low laser slope efficiency reflects the involvement of other non-radiative processes that seriously degrades the ~ 2 μm laser slope efficiency. These non-radiative unwanted processes need to be thoroughly researched in order to develop strategies to suppress them to achieve high laser slope efficiencies. In terms of Yb^{3+}/Ho^{3+} co-doped GPGN glass, the spectroscopically estimated QE at ~ 2.1 μm is ~ 76% while the simulated laser slope efficiency is ~ 20% which reflects the capability of GPGN glass to be utilized for lasing applications above 2 μm.

Another important factor that determines the lasing potential of a gain medium is its emission cross-section at the laser wavelength. It can be observed from Table 6 that the highest peak emission cross-section, σ_{ems}, for $^5I_7$ absorption band of Ho^{3+} estimated in a co-doped lead-silicate glass, Er^{3+}/Ho^{3+}: SPKBEH is ~ 8×10^{-21} cm^2 while the lowest value of ~ 3.5×10^{-21} cm^2 is estimated for a Ho^{3+}: ZBYA fluoride glass. Multiple factors affect the emission cross section of $^5I_7$ band of Ho^{3+} e.g., radiative lifetime of the laser ion in a specific sample, thermal loading effects on the sample, its refractive index, technique through which the cross section is measured etc. σ_{ems} for SPKBEH2 in Table 2 is measured using Mc-Cumber equation given by Eq. (1):

$$\sigma_{abs} = \sigma_{ems}(v)\exp\left(\frac{hv - E_0}{k_B T}\right) \qquad (1)$$

σ_{abs} in the above equation represents the absorption cross-section that can be estimated using the formula $\sigma_{abs}(\lambda) = \frac{2.303D(\lambda)}{NL}$, where D ($\lambda$) is the optical density extracted from the absorption spectrum, N is the ion density of the dopant ions and L is the length of the transmission path, ν is the emission frequency, E_0 is the energy of a specific energy level, Boltzmann constant is represented by k_B and T is the temperature in Kelvins. For all the other glasses except Er^{3+}/Ho^{3+}: SPKBEH 2 in Table 6, σ_{ems} is estimated utilizing the Füchtbauer–Ladenburg expression given by Eq. (2)

$$\sigma_{ems}(\lambda) = \frac{\lambda^4}{8\pi c n^2 \tau_r} \cdot \frac{I(\lambda)}{\int I(\lambda)d(\lambda)} \qquad (2)$$

τ_r in the above expression is the evaluated fluorescence lifetime of $^5I_7$, n represents the refractive index of the active material, c is the speed of light, λ is the transition wavelength, and I(λ) is the fluorescence intensity function. Elevated levels of σ_{ems} reflect higher proportions of other non-radiative processes that directly affect the fluorescence lifetime of $^5I_7$ energy level (indirect relation between σ_{ems} and τ_r [54]). These non-radiative processes, normally arising due to high phonon energy of the glasses, including complex processes such as the up conversion (UC), excited state absorption (ESA), multi-phonon relaxation to the lower energy state and also

Table 6
Spectroscopic properties of $^5I_7$ absorption band of Ho^{3+} in various glasses.

Glass material	Measured lifetime (τ_m - ms)	Radiative lifetime (τ_r - ms)	Peak Absorption cross -section (cm^2)	Peak Emission cross section (cm^2)	QE = $\tau_m \times A_r$	Ref.
SPANK (silicate) (Ho^{3+})	1.31	15.4	3.95×10^{-21}	3.05×10^{-21}	6%	[16]
SPKBEH 2 (silicate) Er^{3+}/ Ho^{3+}	0.88	11.28	3.50×10^{-21}	8.00×10^{-21}	7.8%	[43]
SBL silicate glass (Ho^{3+}/ Yb^{3+})	not known	12.7	2.36×10^{-21}	5.05×10^{-21}	–	[42]
Yb^{3+}/Ho^{3+}: GPGN (germanate)	7.74	10.1	4.20×10^{-21}	4.20×10^{-21}	76%	[54]
Fluorophosphate	8.3	14.0	5.10×10^{-21}	5.50×10^{-21}	59.3%	[25]
ZBYA fluoride	12.1	12.6	–	3.50×10^{-21}	96%	[46]

the absorption due to the presence of the hydroxyl groups. The materials with higher phonon energies usually have lower $^5I_7$ fluorescence lifetime compared to their radiative lifetimes. To achieve higher laser slope efficiencies, the fluorescence lifetime of the metastable energy state ($^5I_7$ for ~ 2.1 μm) is expected to be longer as it contributes to population inversion during laser operation. Moreover, longer lifetimes are favorable for Q-switched laser operations where energy is accumulated in the laser cavity to achieve intense nano-scale laser pulses. Phonon energy is therefore an important indicator of glass material to be considered for laser applications.

A few of the important spectroscopic properties of $^5I_8 \rightarrow {}^5I_7$ transition of Ho^{3+} in various transparent glassy materials are presented in Table 6. These parameters include the radiative lifetime of $^5I_7$ energy state of Ho^{3+}, pumping wavelength λ_P, its peak emission wavelength σ_{ems}, peak absorption cross section σ_{abs} and the achievable quantum efficiency. It is observed from Table 6 that there is a large difference between the spectroscopically estimated radiative lifetime τ_r (inverse of the spontaneous transition probability (A_r) of Ho^{3+}: $^5I_7$ and its experimentally measured fluorescence lifetime (τ_m). This large difference is due to the high phonon energy of the silica glass that increases non-radiative losses in the sample at ~ 2 μm and results in its low quantum efficiency (~ 8%) (QE = $\tau_m \times A_r$). On the other hand, Yb^{3+}/Ho^{3+}: GPGN glass shows high quantum efficiency as the difference between τ_r and τ_m is not that large due to low phonon energy of the GPGN glass (~ 800 cm^{-1}).

Some exotic glasses such as Nd^{3+}:$Ba(PO_3)_2$ + La_2O_3 (PBaLa) glass in Ref. [93] are also claimed to be attractive alternatives for spectral region >2 μm. The conclusion is based on promising values of characteristic parameters in the glass i.e., σ_{ems}, τ_r and quantum efficiency. Similarly, boro-bismuth glasses as in Ref. [94] are considered in the same category of promising options for short to mid-IR spectral region. However, the spectroscopic properties (using Judd-Ofelt analysis) of both these glasses have been studied for Nd^{3+} and more experimental evidence are required in the mid-IR spectral region to validate the claim. In contrast to these exotic glasses, the fluoride glasses (such as ZBYA and ZBLAN) are attractive gain media for laser applications above ~ 2.1 μm as they possess high quantum efficiency (theoretical and experimental) of Ho^{3+} in spectral region > 2.1 μm [46]. However, only fiber lasers and waveguide lasers have been investigated in these glasses in spectral region above 2.1 μm and no solid-state bulk lasers have been realized. This is because ZBYA and ZBLAN are not successful glasses for bulk laser operation as they possess negative thermo-optic property and results in negative thermal lensing effects in the sample, abstaining the glass to produce stable laser oscillations in the laser cavity.

3.3. ~ 2.1 μm laser action in Ho^{3+} doped GPGN glass

In this segment we briefly present our contribution to the development of a small cavity microchip laser operation in a Ho^{3+} doped GPGN glass that operates at 2095 nm. The molar composition used for ~ 2.1 μm microchip laser is 55GeO$_2$-31PbO-4Ga$_2$O$_3$–9Na$_2$O–Ho$_2$O$_3$. The absorption of Ho^{3+} doped glass reveals peak absorption cross-section of ~ 4.5×10^{-21} cm^2 for the $^5I_7$ absorption band of Ho^{3+} (estimated using Beer-Lambert law) (Fig. 5(a)). On the contrary, the peak emission cross-section of Ho^{3+} at ~ 2.1 μm, when pumped with a 1.94 μm Tm^{3+} fiber laser, is ~ 5.5×10^{-21} cm^2 (computed using Füchtbauer–Ladenburg equation) (Fig. 5 (a)). The fluorescence decay curve for $^5I_7$ energy state of Ho^{3+} in GPGN is presented in Fig. 5(b). The exponential decay in the fluorescence curve indicates the lifetime of $^5I_7$ energy state to be 8.11 ms (long enough to consider GPGN glass promising for Q-switched pulsed laser operation). These optical properties of Ho^{3+} in GPGN glass are presented in Table 7.

In-band pumping of Ho^{3+} using a 1.94 μm Tm^{3+} fiber laser is utilized to induce ~ 2.1 μm laser oscillations in a 4.8 mm long bulk Ho^{3+}: GPGN sample. The laser cavity is a simple Fabry-Perot construction comprising of the bulk Ho^{3+}: GPGN glass sandwiched between two plane mirrors acting as input and output couplers. The input coupler utilized in the setup has > 99% transmission at 1.94 μm while highly reflecting properties at ~ 2.1 μm to confine almost all the ~ 2.1 μm laser oscillations within the bulk Ho^{3+}: GPGN glass. The output coupler transmits only 5% of the laser oscillations and is highly transmitting for the pump laser which is filtered out to obtain the continuous wave single frequency ~ 2.1 μm laser operation in Ho^{3+} in GPGN glass. To the best of our knowledge this is the first single frequency small cavity ~ 2.1 μm bulk laser demonstrated in a GPGN glass generating a laser slope efficiency of up to ~ 20% at a peak operating wavelength of 2095 nm (Fig. 6(a)). The FWHM spectral width of the laser is ~ 8 nm (Fig. 6(b)).

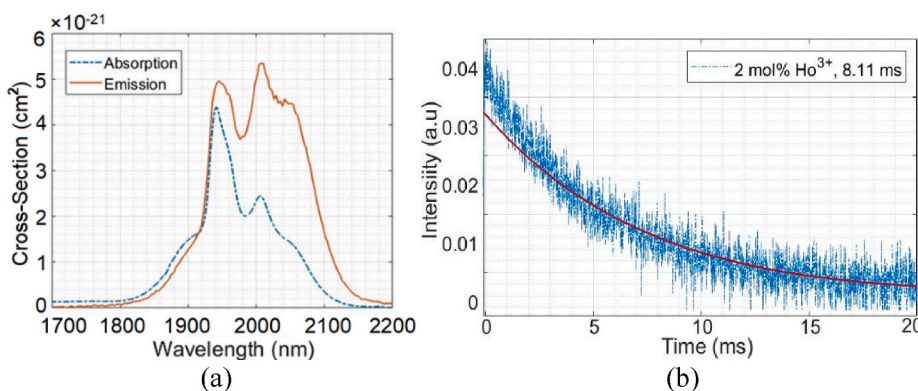**Fig. 5.** (a) Absorption and emission cross-section of 2.6 wt% of Ho^{3+} in GPGN (b) Fluorescence decay curve of $^5I_7$: Ho^{3+} in GPGN for 2.6 wt% of Ho^{3+}.

Table 7

$\sim$ 2.1 μm laser properties of Ho^{3+} in GPGN glass. σ_{abs} is the peak absorption cross section of $^5I_7$ absorption band of Ho^{3+}; τ_r is the measured fluorescence lifetime of $^5I_7$ energy state; σ_{ems} is the peak emission cross-section, λ_p is the pump wavelength; λ_s is the signal wavelength, P_{th} is the laser threshold power; FWHM is full width half maximum laser spectral width; η_s is the laser slope efficiency.

Glass material	Ho^{3+} concentration	σ_{abs} (cm^2)	τ_r (ms)	σ_{ems} (cm^2)	λ_p (nm)	λ_s (nm)	FWHM (nm)	P_{th} (mW)	η_s (%)
Ho^{3+}: GPGN (GeO$_2$-PbO-Ga$_2$O$_3$–Na$_2$O)	2.6 wt%	4.4×10^{-21}	8.11	5.5×10^{-21}	1945	2095	8	100	20

In-depth spectroscopic analysis of Ho^{3+} in GPGN glass, the detailed $\sim$ 2.1 μm laser operation and the factors effecting the Ho^{3+} laser slope efficiency in GPGN is not the scope of this paper and is therefore not included. We aim to soon publish the detailed information on this new discovery, however, a few of the highlights on the major properties Ho^{3+}: GPGN bulk laser are given in Table 7.

The efficiency of $\sim$ 2.1 μm laser operation can be increased by co-doping the GPGN glass with a sensitizer ion such as Yb^{3+}, Er^{3+}, Nd^{3+} or Tm^{3+}. Yb^{3+} has strong absorption at 976 nm (absorption cross-section $\sim 1.1 \times 10^{-20}$ cm^2 [54]), where high power laser diodes are readily accessible and are relatively inexpensive. Selecting Tm^{3+} in place of Yb^{3+} might have other advantages such as higher efficiencies because of the so called cross-relaxation process due to which Tm^{3+} is considered as the most efficient sensitizer ion so far for Ho^{3+} for $\sim$ 2.1 μm laser emission. However, Tm^{3+} co-doped system requires 790 nm LD pumping as it has strong absorption up to 795 nm. Single mode LDs operating at 790 nm are required to launch efficiently in the core of the waveguide for laser transition. These single mode 790 nm pump sources are although commercially available but are expensive and have low output powers (e.g., <250 mW from Thorlabs). Laser threshold in germanate is usually > 0.2 W and requires high power pump sources.

In contrast to 790 nm LDs, 808 nm LDs are comparatively high-power single mode sources which are normally designed to pump Nd^{3+} doped systems. However the absorption of Tm^{3+} at 808 nm is weaker and requires higher concentrations to be doped into the glass to achieve the required absorption to induce population inversion for the required laser transition. To efficiently utilize 808 nm high power single mode LD, Nd^{3+} can also be used to sensitize Ho^{3+} as evidenced in a modified silicate glass (oxyfluoride silicate). However, the theoretical energy transmission efficiency achieved from Nd^{3+} to Ho^{3+} in Ref. [95] is only 50%.

Er^{3+} is also an option to be used to sensitize Ho^{3+} as reported in a study in Ref. [43] where 89% of energy transfer efficiency is achieved from Er^{3+} to Ho^{3+} when excited with a 976 nm pump source. However, the several energy states of Er^{3+} have the tendency to promote the undesirable non-radiative processes (up-conversion, excited state absorption and multi-phonon relaxation) in GPGN. 980 nm pumped tri-doped systems have also been investigated in different glasses for efficient luminescence at $\sim$ 2 μm. For example, in a recent study on tellurite glass (HMO glass) Er^{3+} and Yb^{3+} are both used to sensitize Ho^{3+} where the authors claim to achieve 93% more luminescence at $\sim$ 2.1 μm when pumped with 980 nm compared to co-doped systems. This tri-doped system although theoretically is promising, however, for a GPGN glass whose phonon energy is slightly greater ($\sim$ 800 cm^{-1}) than tellurite glass ($\sim$ 750 cm^{-1}) the system can become complicated due to higher multi-phonon decay rate.

4. Conclusion

This review article represents the potential of a germanate glass (GPGN) for its utility in laser applications around 2.1 μm. A comparison of the spectroscopic properties of GPGN with other germanates and commercially available silica and fluoride glasses is presented in the article to evaluate its lasing capability for $\sim$ 2.1 μm. In contrast to other germanate glasses, GPGN glass comprises of high emission cross section at $\sim$ 2.1 μm, lower multiphonon decay rates, higher energy transfer efficiency (in case of co-doped GPGN), higher gain and good quantum efficiency. The near infrared lasing attributes of as made GPGN glass are demonstrated earlier by the authors in Refs. [55,56,96]. The cumulative impact of these results reflects GPGN glass as a high potential laser gain medium for $\sim$ 2.1 μm applications by realizing the continuous wave single frequency laser action in a short cavity (5 mm) Ho^{3+} doped GPGN glass. The laser operates at peak laser wavelength of 2095 nm and the attained laser slope efficiency is $\sim$ 20%. The obtained laser slope efficiency is although very promising, however, for high power laser applications beyond 2 μm, further modifications to the glass composition is required to reduce its phonon energy in order to suppress the non-radiative processes within GPGN (e.g., addition of halides in the GPGN glass, provided its thermal stability is not impacted). Moreover, the glass contains higher amount of OH groups around 2.3 μm and from 2.8 μm to 3.5 μm. The presence of these OH groups further deteriorate the laser performance above $\sim$ 2.1 μm region. These OH groups need to be mitigated during the glass fabrication process to enhance its lasing performance for longer wavelengths.

Author contribution statement

Funding statement
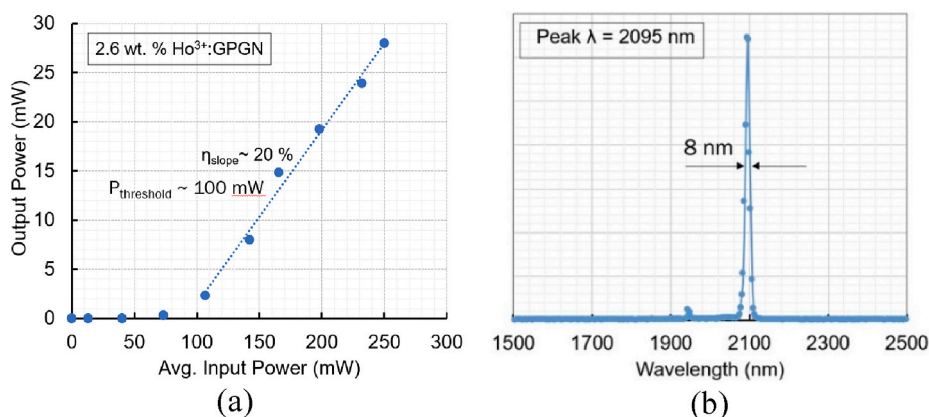
Fig. 6. (a) Ho^{3+} laser operation in bulk GPGN with 20% laser slope efficiency (b) Ho^{3+}: GPGN operation with peak at ~ 2.1 μm. Small peak at 1.94 μm is the pump wavelength leaking from the output coupler.

Data availability statement

Data included in article/supp. material/referenced in article

Declaration of interest's statement

The authors declare no competing interests.

Acknowledgments

References

[1] X. Lin, S. Yang, 2 um eye-safe solar-pumped laser, in: High-Power Lasers and Applications XI, SPIE, 2020, pp. 83–94.
[2] J. Shi, H. Wang, J. Qian, X. He, Investigations on thermal-transfer characteristics of water based on stimulated Brillouin scattering, Opt Commun. 363 (2016) 21–25.
[3] K. Scholle, S. Lamrini, P. Koopmann, P. Fuhrberg, 2 μm laser sources and their possible applications, in: Frontiers in Guided Wave Optics and Optoelectronics, IntechOpen, 2010.
[4] J. Houghton, The Physics of Atmospheres, Cambridge University Press, 2002.
[5] R. Xu, J. Pan, L. Hu, J. Zhang, 2.0 μ m emission properties and energy transfer processes of Yb^{3+}/Ho^{3+} codoped germanate glass, J. Appl. Phys. 108 (2010), 043522.
[6] M. Kochanowicz, J. Żmojda, P. Miluski, A. Baranowska, T. Ragin, J. Dorosz, M. Kuwik, W.A. Pisarski, J. Pisarska, M. Lesniak, 2 μm emission in gallo-germanate glasses and glass fibers co-doped with Yb3+/Ho3+ and Yb3+/Tm3+/Ho3+, J. Lumin. 211 (2019) 341–346.
[7] M. Chen, W. Li, S. Ji, X. Lin, X. Zhan, H. Xu, Z. Cai, Study on fluorescence characteristics of the Ho3+: ZBLAN fiber under~ 640 nm excitation, Opt. Mater. 97 (2019), 109351.
[8] Z. Jun, D. Shi-Xun, P. Bo, X. Tie-Feng, W. Xun-Si, Z. Xiang-Hua, Mid-infrared Emission Properties of Ho3+-Doped Ge-Ga-S-CsI Glasses, 2010.
[9] X. Yang, W. Wang, Q. Zhang, BaF2 modified Cr3+/Ho3+ co-doped germanate glass for efficient 2.0 μm fiber lasers, J. Non-Cryst. Solids 482 (2018) 147–153.
[10] D. Li, W. Xu, P. Kuan, W. Li, Z. Lin, X. Wang, L. Zhang, C. Yu, K. Li, L. Hu, Spectroscopic and laser properties of Ho3+ doped lanthanum-tungsten-tellurite glass and fiber, Ceram. Int. 42 (2016) 10493–10497.
[11] S.D. Jackson, Towards high-power mid-infrared emission from a fibre laser, Nat. Photonics 6 (2012) 423–431.
[12] A. Tunnermann, T. Schreiber, F. Roser, A. Liem, S. Hofer, H. Zellmer, S. Nolte, J. Limpert, The renaissance and bright future of fibre lasers, J. Phys. B Atom. Mol. Opt. Phys. 38 (2005) S681.
[13] Y. Lee, Evaluating subsurface damage in optical glasses, J. Europ. Opt. Soc. Rapid Publ. 6 (2011).
[14] F. Todorov, J. Aubrecht, P. Peterka, O. Schreiber, A.A. Jasim, J. Mrazek, O. Podrazký, M. Kamradek, N. Kanagaraj, M. Grabner, Active optical fibers and components for fiber lasers emitting in the 2-μm spectral range, Materials 13 (2020) 5177.
[15] E. Migal, E. Mareev, E. Smetanina, G. Duchateau, F. Potemkin, Role of wavelength in photocarrier absorption and plasma formation threshold under excitation of dielectrics by high-intensity laser field tunable from visible to mid-IR, Sci. Rep. 10 (2020) 1–10.
[16] X. Liu, P. Kuan, D. Li, S. Gao, X. Wang, L. Zhang, L. Hu, D. Chen, Heavily Ho 3+-doped lead silicate glass fiber for~ 2 μm fiber lasers, Opt. Mater. Express 6 (2016) 1093–1098.
[17] J. Li, Z. Sun, H. Luo, Z. Yan, K. Zhou, Y. Liu, L. Zhang, Wide wavelength selectable all-fiber thulium doped fiber laser between 1925 nm and 2200 nm, Opt Express 22 (2014) 5387–5399.
[18] S.D. Jackson, A. Sabella, A. Hemming, S. Bennetts, D.G. Lancaster, High-power 83 W holmium-doped silica fiber laser operating with high beam quality, Opt. Lett. 32 (2007) 241–243.
[19] K. Saito, M. Yamaguchi, H. Kakiuchida, A. Ikushima, K. Ohsono, Y. Kurosawa, Limit of the Rayleigh scattering loss in silica fiber, Appl. Phys. Lett. 83 (2003) 5175–5177.
[20] C.R. Kurkjian, P.K. Gupta, R.K. Brow, The strength of silicate glasses: what do we know, what do we need to know? Int. J. Appl. Glass Sci. 1 (2010) 27–37.
[21] R. Sajzew, R. Limbach, L. Wondraczek, Deformation and fracture of silica glass fiber under sharp wedge-indentation, Front Mater 7 (2020).

[22] T. Wang, F. Huang, Q. Qi, Y. Tian, J. Zhang, S. Xu, Spectroscopic properties and energy transfer process in Tm3+-doped Silica-germanate glasses, J. Lumin. 187 (2017) 205–210.

[23] X. Fan, P. Kuan, K. Li, L. Zhang, D. Li, L. Hu, Spectroscopic properties and quenching mechanism of 2 μm emission in Ho3+ doped germanate glasses and fibers, Opt. Mater. Express 5 (2015) 1356–1365.

[24] J. Xia, Y. Tian, B. Li, L. Zheng, X. Jing, J. Zhang, S. Xu, Enhanced 2.0 μm emission in Ho3+/Yb3+ co-doped silica-germanate glass, Infrared Phys. Technol. 81 (2017) 17–20.

[25] O. Bentouila, K. Aiadi, F. Rehouma, M. Poulain, F. Benhbirech, Thermal stability and spectroscopic study of Ho3+/Yb3+ co-doped fluorophosphates glasses, J. King Saud Univ. Sci. 31 (2019) 628–634.

[26] X. Zhu, N. Peyghambarian, High-power ZBLAN glass fiber lasers: review and prospect, Adv. Optoelectron. (2010) 2010.

[27] H.A. Sidek, H.R. Bahari, M.K. Halimah, W.M. Yunus, Preparation and elastic moduli of germanate glass containing lead and bismuth, Int. J. Mol. Sci. 13 (2012) 4632–4641.

[28] G.-P. Su, L. Qiu, X.-H. Zheng, Z.-H. Xiao, D.-W. Tang, Effective thermal-conductivity measurement on germanate glass–ceramics employing the $ 3\omega $ ω method at high temperature, Int. J. Thermophys. 35 (2014) 336–345.

[29] V. Vazhenin, A. Potapov, M.Y. Artyomov, A. Vylkov, Paramagnetic copper centers in ferroelectric lead germanate with halogens, Phys. Solid State 56 (2014) 1610–1614.

[30] V. Denisov, S. Tinkova, L. Denisova, L. Irtyugo, Thermal conductivity of the PbGeO 3 and PbGe 3 O 7 glasses, Phys. Solid State 53 (2011) 2025–2027.

[31] H.T. Munasinghe, A. Winterstein-Beckmann, C. Schiele, D. Manzani, L. Wondraczek, S. Afshar, T.M. Monro, H. Ebendorff-Heidepriem, Lead-germanate glasses and fibers: a practical alternative to tellurite for nonlinear fiber applications, Opt. Mater. Express 3 (2013) 1488–1503.

[32] S. Tokita, M. Murakami, S. Shimizu, M. Hashida, S. Sakabe, Liquid-cooled 24 W mid-infrared Er: ZBLAN fiber laser, Opt. Lett. 34 (2009) 3062–3064.

[33] H. Gu, Z. Qin, G. Xie, T. Hai, P. Yuan, J. Ma, L. Qian, Generation of 131 fs mode-locked pulses from 2.8 μm Er: ZBLAN fiber laser, Chin. Opt. Lett. 18 (2020), 031402.

[34] R. Woodward, M. Majewski, N. Macadam, G. Hu, T. Albrow-Owen, T. Hasan, S. Jackson, Q-switched Dy: ZBLAN fiber lasers beyond 3 μm: comparison of pulse generation using acousto-optic modulation and inkjet-printed black phosphorus, Opt Express 27 (2019) 15032–15045.

[35] D. Lancaster, V. Stevens, V. Michaud-Belleau, S. Gross, A. Fuerbach, T. Monro, Holmium-doped 2.1 μm waveguide chip laser with an output power> 1 W, Opt Express 23 (2015) 32664–32670.

[36] R. Woodward, M. Majewski, G. Bharathan, D. Hudson, A. Fuerbach, S. Jackson, Watt-level dysprosium fiber laser at 3.15 μm with 73% slope efficiency, Opt. Lett. 43 (2018) 1471–1474.

[37] D.G. Lancaster, S. Gross, H. Ebendorff-Heidepriem, A. Fuerbach, M.J. Withford, T. Monro, 2.1 μm waveguide laser fabricated by femtosecond laser direct-writing in Ho 3+, Tm 3+: ZBLAN glass, Opt. Lett. 37 (2012) 996–998.

[38] D. Lancaster, S. Gross, M. Withford, T. Monro, Widely tunable short-infrared thulium and holmium doped fluorozirconate waveguide chip lasers, Opt Express 22 (2014) 25286–25294.

[39] P. Guay, N.B. Hebert, J. Genest, D.G. Lancaster, Versatile waveguide chip laser for 2.9 μm emission, in: 2019 Conference on Lasers and Electro-Optics Europe & European Quantum Electronics Conference (CLEO/Europe-EQEC), IEEE, 2019, p. 1.

[40] O. Henderson-Sapir, A. Malouf, N. Bawden, J. Munch, S.D. Jackson, D.J. Ottaway, Recent advances in 3.5 *μ*m erbium-doped mid-infrared fiber lasers, IEEE J. Sel. Top. Quant. Electron. 23 (2017) 6–14.

[41] R. Cao, M. Cai, Y. Lu, Y. Tian, F. Huang, S. Xu, J. Zhang, Ho3+/Yb3+ codoped silicate glasses for 2 μm emission performances, Appl. Opt. 55 (2016) 2065–2070.

[42] R. Cao, M. Cai, Y. Lu, Y. Tian, F. Huang, S. Xu, J. Zhang, Ho 3+/Yb 3+ codoped silicate glasses for 2 μm emission performances, Appl. Opt. 55 (2016) 2065–2070.

[43] G. Qian, G. Tang, Z. Shi, L. Jiang, K. Huang, J. Gan, D. Chen, Q. Qian, F. Tu, H. Tao, Efficient 2 μm emission in Er3+/Ho3+ co-doped lead silicate glasses under different excitations, Opt. Mater. 82 (2018) 147–153.

[44] X. Jiang, J. Lousteau, B. Richards, A. Jha, Investigation on germanium oxide-based glasses for infrared optical fibre development, Opt. Mater. 31 (2009) 1701–1706.

[45] P.K. Mishra, K. Singh, A. Upadhyay, H. Kumar, Compositional dependence of thermal transport and optical properties of Se85 Ge15-x Pbx (0≤ x≤ 10) chalcogenide glassy alloys, Opt. Mater. 97 (2019), 109395.

[46] H. Ebendorff-Heidepriem, I. Szabo, Z. Rasztovits, Crystallization behavior and spectroscopic properties of Ho3+-doped ZBYA-fluoride glass, Opt. Mater. 14 (2000) 127–136.

[47] L. Wetenkamp, G. West, H. Tobben, Optical properties of rare earth-doped ZBLAN glasses, J. Non-Cryst. Solids 140 (1992) 35–40.

[48] D.G. Lancaster, S. Gross, H. Ebendorff-Heidepriem, M.J. Withford, T.M. Monro, S.D. Jackson, Efficient 2.9 μm fluorozirconate glass waveguide chip laser, Opt. Lett. 38 (2013) 2588–2591.

[49] D. Lancaster, S. Gross, M. Withford, T.M. Monro, Widely tunable short-infrared thulium and holmium doped fluorozirconate waveguide chip lasers, Opt Express 22 (2014) 25286–25294.

[50] D. Lancaster, S. Gross, H. Ebendorff-Heidepriem, K. Kuan, T. Monro, M. Ams, A. Fuerbach, M. Withford, Fifty percent internal slope efficiency femtosecond direct-written Tm 3+: ZBLAN waveguide laser, Opt. Lett. 36 (2011) 1587–1589.

[51] D. Lancaster, S. Gross, A. Fuerbach, H.E. Heidepriem, T. Monro, M. Withford, Versatile large-mode-area femtosecond laser-written Tm: ZBLAN glass chip lasers, Opt Express 20 (2012) 27503–27509.

[52] X. Wang, P. Zhou, Y. He, Z. Zhou, Erbium silicate compound optical waveguide amplifier and laser [Invited], Opt. Mater. Express 8 (2018) 2970–2990.

[53] D. Lancaster, S. Gross, S. Ng, H. Ebendorff-Heidepriem, T. Monro, A. Fuerbach, M. Withford, A new class of 2μm waveguide lasers produced by fs direct-writing of Tm3+ and Ho3+ doped ZBLAN glass, in: Conference on Lasers and Electro-Optics/Pacific Rim, Optical Society of America, 2011, p. C888.

[54] M. Khalid, D. Lancaster, H. Ebendorff-Heidepriem, Spectroscopic analysis and laser simulations of Yb 3+/Ho 3+ co-doped lead-germanate glass, Opt. Mater. Express 10 (2020) 2819–2833.

[55] M. Khalid, Broadband fluorescence emission and laser demonstration in large mode waveguide structure in Yb3+ doped germanate glass, Opt. Appl. 51 (2021).

[56] M. Khalid, G.Y. Chen, J. Bei, H. Ebendorff-Heidepriem, D.G. Lancaster, Microchip and ultra-fast laser inscribed waveguide lasers in Yb3+germanate glass, Opt. Mater. Express 9 (2019) 3557–3564.

[57] O. Henderson-Sapir, A. Malouf, N. Bawden, J. Munch, S.D. Jackson, D.J. Ottaway, Recent advances in 3.5 μm erbium-doped mid-infrared fiber lasers, IEEE J. Sel. Top. Quant. Electron. 23 (2016) 6–14.

[58] J. Pisarska, M. Soltys, A. Gorny, M. Kochanowicz, J. Zmojda, J. Dorosz, D. Dorosz, M. Sitarz, W.A. Pisarski, Rare earth-doped barium gallo-germanate glasses and their near-infrared luminescence properties, Spectrochim. Acta Mol. Biomol. Spectrosc. 201 (2018) 362–366.

[59] J. Siegel, J.M. Fernandez-Navarro, A. Garcia-Navarro, V. Diez-Blanco, O. Sanz, J. Solis, F. Vega, J. Armengol, Waveguide structures in heavy metal oxide glass written with femtosecond laser pulses above the critical self-focusing threshold, Appl. Phys. Lett. 86 (2005) 121109.

[60] C.B. De Araujo, D. Silverio da Silva, T.A. Alves de Assumpção, L.R.P. Kassab, D. Mariano da Silva, Enhanced optical properties of germanate and tellurite glasses containing metal or semiconductor nanoparticles, Sci. World J. 2013 (2013).

[61] S. Cui, R. Chahal, C. Boussard-Pledel, V. Nazabal, J.L. Doualan, J. Troles, J. Lucas, B. Bureau, From selenium- to tellurium-based glass optical fibers for infrared spectroscopies, Molecules 18 (2013) 5373–5388.

[62] V. Kamynin, A. Kurkov, V. Mashinsky, Supercontinuum generation up to 2.7 μm in the germanate-glass-core and silica-glass-cladding fiber, Laser Phys. Lett. 9 (2012) 219–222.

[63] B. Richards, T. Teddy-Fernandez, G. Jose, D. Binks, A. Jha, Mid-IR (3–4 μm) fluorescence and ASE studies in Dy3+ doped tellurite and germanate glasses and a fs laser inscribed waveguide, Laser Phys. Lett. 10 (2013), 085802.

[64] S.S. Bayya, G.D. Chin, J.S. Sanghera, I.D. Aggarwal, Germanate glass as a window for high energy laser systems, Opt Express 14 (2006) 11687–11693.

[65] J. Wu, Z. Yao, J. Zong, S. Jiang, Highly efficient high-power thulium-doped germanate glass fiber laser, Opt. Lett. 32 (2007) 638–640.

[66] J. Geng, J. Wu, S. Jiang, J. Yu, Efficient single-frequency thulium doped fiber laser near 2-μm, in: Advanced Solid-State Photonics, Optical Society of America, 2007, p. WE4.

[67] S.D. Jackson, D.G. Lancaster, Fiber Lasers that Bridge the Shortwave to Midwave Regions of the Infrared Spectrum, 2012.

[68] A.B. Seddon, Z. Tang, D. Furniss, S. Sujecki, T.M. Benson, Progress in rare-earth-doped mid-infrared fiber lasers, Opt Express 18 (2010) 26704–26719.

[69] J. Ballato, H. Ebendorff-Heidepriem, J. Zhao, L. Petit, J. Troles, Glass and process development for the next generation of optical fibers: a review, Fibers 5 (2017) 11.

[70] X. Wen, G. Tang, J. Wang, X. Chen, Q. Qian, Z. Yang, Tm 3+ doped barium gallo-germanate glass single-mode fibers for 2.0 μm laser, Opt Express 23 (2015) 7722–7731.

[71] T. Wei, Y. Tian, F. Chen, M. Cai, J. Zhang, X. Jing, F. Wang, Q. Zhang, S. Xu, Mid-infrared fluorescence, energy transfer process and rate equation analysis in Er 3 + doped germanate glass, Sci. Rep. 4 (2014) 1–10.

[72] M. Cai, B. Zhou, F. Wang, Y. Tian, J. Zhou, S. Xu, J. Zhang, Highly efficient mid-infrared 2 μm emission in Ho 3+/Yb 3+-codoped germanate glass, Opt. Mater. Express 5 (2015) 1431–1439.

[73] G. Bai, L. Tao, K. Li, L. Hu, Y.H. Tsang, Enhanced light emission near 2.7 μm from Er–Nd co-doped germanate glass, Opt. Mater. 35 (2013) 1247–1250.

[74] L. Qiongfei, X. Haiping, Y. Zhang, W. Jinhao, J. Zhang, H. Sailong, Gain properties of germanate glasses singly doped with Tm3+ and Ho3+ ions, J. Rare Earths 27 (2009) 76–82.

[75] W. Wang, B. Zhou, S. Xu, Z. Yang, Q. Zhang, Recent advances in soft optical glass fiber and fiber lasers, Prog. Mater. Sci. 101 (2019) 90–171.

[76] A. Kurkov, V. Dvoyrin, A. Marakulin, All-fiber 10 W holmium lasers pumped at λ= 1.15 μm, Opt. Lett. 35 (2010) 490–492.

[77] X. Wang, P. Zhou, Y. Miao, H. Zhang, H. Xiao, X. Wang, Z. Liu, Raman fiber laser-pumped high-power, efficient Ho-doped fiber laser, JOSA B 31 (2014) 2476–2479.

[78] A.S. Kurkov, E.M. Sholokhov, V.B. Tsvetkov, A.V. Marakulin, L. Minashina, O.I. Medvedkov, A.F. Kosolapov, Holmium fibre laser with record quantum efficiency, Quant. Electron. 41 (2011) 492.

[79] Y. Li, Y. Zhao, B. Ashton, S. Jackson, S. Fleming, Highly efficient and wavelength-tunable Holmium-doped silica fibre lasers, in: 2005 31st European Conference on Optical Communication, ECOC 2005, IET, 2005, pp. 679–680.

[80] A. Hemming, N. Simakov, M. Oermann, A. Carter, J. Haub, Record efficiency of a holmium-doped silica fibre laser, in: 2016 Conference on Lasers and Electro-Optics (CLEO), IEEE, 2016, pp. 1–2.

[81] A. Hemming, S. Bennetts, N. Simakov, A. Davidson, J. Haub, A. Carter, High power operation of cladding pumped holmium-doped silica fibre lasers, Opt Express 21 (2013) 4560–4566.

[82] A. Sincore, L. Shah, V. Smirnov, M. Richardson, Comparison of in-band pumped Tm: fiber and Ho: fiber, in: Fiber Lasers XIII: Technology, Systems, and Applications, International Society for Optics and Photonics, 2016, p. 97280S.

[83] P.-W. Kuan, X. Fan, X. Li, D. Li, K. Li, L. Zhang, C. Yu, L. Hu, High-power 2.04 μm laser in an ultra-compact Ho-doped lead germanate fiber, Opt Lett. 41 (2016) 2899–2902.

[84] X. Fan, P. Kuan, K. Li, L. Zhang, D. Li, L. Hu, Spectroscopic properties and quenching mechanism of 2 μm emission in Ho 3+ doped germanate glasses and fibers, Opt. Mater. Express 5 (2015) 1356–1365.

[85] F.B. Slimen, S. Chen, J. Lousteau, Y. Jung, N. White, S. Alam, D.J. Richardson, F. Poletti, Highly efficient Tm 3+ doped germanate large mode area single mode fiber laser, Opt. Mater. Express 9 (2019) 4115–4125.

[86] J. Wu, Z. Yao, J. Zong, A. Chavez-Pirson, N. Peyghambarian, J. Yu, Single-frequency fiber laser at 2.05 um based on ho-doped germanate glass fiber, in: Fiber Lasers VI: Technology, Systems, and Applications, International Society for Optics and Photonics, 2009, p. 71951K.

[87] Y. Lu, M. Cai, R. Cao, Y. Tian, F. Huang, S. Xu, J. Zhang, Ho3+ doped germanate-tellurite glass sensitized by Er3+ and Yb3+ for efficient 2.0 μm laser material, Mater. Res. Bull. 84 (2016) 124–131.

[88] R. Xu, M. Wang, Y. Tian, L. Hu, J. Zhang, 2.05 μm emission properties and energy transfer mechanism of germanate glass doped with Ho3+, Tm3+, and Er3+, J. Appl. Phys. 109 (2011), 053503.

[89] A. Albalawi, M. Kochanowicz, J. Zmojda, P. Miluski, D. Dorosz, S. Taccheo, Fluorescence spectrum of an Yb: Er: Tm: Ho doped germanate glass, in: Advanced Solid State Lasers, Optical Society of America, 2018. ATu2A. 4.

[90] M.C. Falconi, D. Laneve, V. Portosi, S. Taccheo, F. Prudenzano, Modeling of a 980-nm pumped Yb: Er: Tm: Ho co-doped glass device for homogeneous gain and lasing over a 600-nm wavelength interval, in: Advanced Solid State Lasers, Optical Society of America, 2019. JTu3A. 31.

[91] M. Cai, B. Zhou, F. Wang, Y. Tian, J. Zhou, S. Xu, J. Zhang, Highly efficient mid-infrared 2 μm emission in Ho3+/Yb3+-codoped germanate glass, Opt. Mater. Express 5 (2015) 1431–1439.

[92] M. Kochanowicz, J. Zmojda, P. Miluski, A. Baranowska, M. Leich, A. Schwuchow, M. Jäger, M. Kuwik, J. Pisarska, W.A. Pisarski, D. Dorosz, Tm3+/Ho3+ co-doped germanate glass and double-clad optical fiber for broadband emission and lasing above 2 μm, Opt. Mater. Express 9 (2019) 1450–1458.

[93] P. Ramprasad, C. Basavapoornima, S.R. Depuru, C. Jayasankar, Spectral investigations of Nd3+: Ba (PO3) 2+ La2O3 glasses for infrared laser gain media applications, Opt. Mater. 129 (2022), 112482.

[94] K.U. Kumar, P. Babu, C. Basavapoornima, R. Praveena, D.S. Rani, C. Jayasankar, Spectroscopic properties of Nd3+-doped boro-bismuth glasses for laser applications, Phys. B Condens. Matter 646 (2022), 414327.

[95] D. Gelija, D.P.R. Borelli, Efficient 2.0 μm emission in Nd3+/Ho3+ co-doped SiO2-Al2O3-Na2CO3-SrF2-CaF2 glasses for mid-infrared laser applications, Mater. Res. Bull. 103 (2018) 268–278.

[96] M. Khalid, G.Y. Chen, H. Ebendorff-Heidepreim, D.G. Lancaster, Femtosecond laser induced low propagation loss waveguides in a lead-germanate glass for efficient lasing in near to mid-IR, Sci. Rep. 11 (2021) 1–12.